Letter

Reflection parity and space-time parity photonic conservation laws in parametric nonlinear optics

Gavriel Lerner,[1,2,*] Matan Even Tzur,[1,2] Ofer Neufeld,[1,2,3] Avner Fleischer,[4] and Oren Cohen[1,2,5,†]

[1]*Physics Department, Technion – Israel Institute of Technology, Haifa 3200003, Israel*
[2]*Solid State Institute, Technion – Israel Institute of Technology, Haifa 3200003, Israel*
[3]*Max Planck Institute for the Structure and Dynamics of Matter, Hamburg 22761, Germany*
[4]*Chemistry Department, Tel Aviv University, Tel Aviv 6997801, Israel*
[5]*Guangdong Technion-Israel Institute of Technology, Shantou, Guangdong 515063, China*

(Received 28 January 2023; accepted 9 July 2024; published 4 November 2024)

Conservation laws are some of the most generic and useful concepts in physics. In nonlinear optical parametric processes, conservation of photonic energy, momenta and parity often lead to selection rules, restricting the allowed polarization and frequencies of the emitted radiation. Here we present a scheme to derive conservation laws in optical parametric processes in which many photons are annihilated and a single photon is emitted. We first rederive with it the known nonlinear optical conservation laws, and then utilize it to predict and explore conservations of reflection parity and space-time parity. Conservation of *reflection-parity* arises from a generalized reflection symmetry of the polarization in a superspace, analogous to the superspace employed in the study of quasicrystals. Conservation of *space-time parity* similarly arises from space-time reversal symmetry in superspace. We explore these conservation laws numerically in the context of high-harmonic generation and outline experimental setups where they can be tested.

DOI: 10.1103/PhysRevResearch.6.L042034

Photonic conservation laws (PCLs) are very powerful for analyzing processes in nonlinear optics [1], especially deriving selection rules that determine which photonic channels are allowed/forbidden, where the allowed channels satisfy all the PCLs simultaneously [2–8]. For example, in harmonic generation, energy conservation coerces the energy of a generated photon to equate exactly to the total energy of the annihilated photons. Thus, if the pump consists of only photons at angular frequency ω then emission of noninteger harmonics is forbidden. In another example, the simultaneous conservation of energy, parity, and spin angular momentum leads to the selection rule of high-harmonic generation driven by co-propagating, bichromatic ω-2ω pump fields that are circularly polarized with opposite helicity [7,9,10].

Another approach for deriving selection rules in nonlinear optics is by analyzing the static and dynamical symmetries (DSs) of the light-matter system. In the field of nonlinear optics, symmetries are standardly used to determine whether a particular nonlinear process is allowed or forbidden according to the medium's point group [1,11]. Recently, a more general group theory was developed describing the symmetries of the electromagnetic (EM) field's time-dependent polarization [12], and its interaction with matter [10]. Recent studies utilized DSs to predict many new selection rules, both due to microscopic symmetries [13,14], microscopic-macroscopic symmetries [15–19], and symmetries in synthetic dimensions [20,21]. Such DSs and their associated selection rules have been applied to shaping the waveforms of extreme ultraviolet and x-ray radiation emitted from high harmonic generation (HHG) [8,22–24] and have enabled ultrafast symmetry-breaking spectroscopy of molecular- [25,26] and solid orientation [27], molecular symmetries [26], chirality [28–32], imaging of microscopic electric-field distributions [33], and detection of valley asymmetry [34,35] and photocurrents [36]. While the PCL approach for deriving selection rules is often more intuitive, the symmetry approach is more mathematically based and more general, i.e., it leads to selection rules that cannot be derived by PCLs. Such examples include reflection DSs that lead to linearly polarized-only harmonics, and elliptical DSs that lead to conservation of the polarization ellipticity [10]. We are motivated to bridge this gap by deriving more PCLs.

Here, we present a method to derive PCLs, associated with DSs of the pump, in parametric nonlinear optical processes. Note that the term photon is used, even though these PCL do not originate from the quantum nature of light, but from discrete symmetries of the classical field. Our approach is based on superspace representation concept (a representation standardly used in the context of quasicrystals [37]; see Sec. 5 of the Supplemental Material (SM) [38]) and the recent multiscale dynamical symmetries concept [15]. Then, we employ this methodology to derive two more PCLs that were not previously known: reflection parity (RP) and space-time parity (STP). These two PCLs predict the direction and phase, respectively, of emitted linearly polarized harmonics according to the parity of the harmonic generation process. Finally, we explore these PCL numerically in high-harmonic generation.

*Contact author: gavriel@campus.technion.ac.il
†Contact author: oren@technion.ac.il

TABLE I. PCL in parametric nonlinear optical processes, $\sum_n \boldsymbol{q_n \gamma_n} \rightarrow \boldsymbol{\gamma_f}$. Rows 1 to 5 present known PCLs while rows 6 and 7 present reflection parity and space-time parity PCLs. The PCLs in rows 1-3 and 6-7 are derived below, and the PCLs in rows 4-5 are derived in the SM.

	Quantity	PCL	Constraints
1	Energy	$\omega_f = \Sigma_n q_n \omega_n$	$q_n \in \mathbb{Z}$
2	Linear momentum	$\vec{k}_f = \Sigma_n q_n \vec{k}_n$	$\lvert\vec{k}\rvert = n_\omega \omega/c$
3	Orbital angular momenta	$l_f = \Sigma_n q_n l_n$	$l \in \mathbb{Z}$
4	Spin angular momenta	$s_f = \Sigma_n q_n s_n$	$s = \pm 1$
5	Parity	$p_f = \Pi_n p_n^{q_n}$	$p = -1$
6	Reflection parity	$r_f = \Pi_n r_n^{q_n}$	$r = \pm 1$
7	Space-time parity	$u_f = \Pi_n u_n^{q_n}$	$u = \pm 1$

We begin by considering a general nonlinear optical process in which the nonlinear medium is isotropic and stationary and its initial and final states are identical. The driving field consists of N-photon types γ_n, where $n = 1, \ldots, N$, and each photon type corresponds to a particular frequency and polarization. The type of the emitted photon is denoted by γ_f (where γ_f is different from all γ_n). Within this picture the nonlinear process may be represented by the following photonic reaction equation:

$$\sum_n q_n \gamma_n \rightarrow \gamma_f, \tag{1}$$

in which q_n is the number of driver photons of type γ_n that are annihilated (or generated when q_n is negative) in the generation of a photon of type γ_f.

The known PCLs of these processes are given in rows 1–5 in Table I. Rows 6 and 7 present our derived PCL. All seven PCLs will be derived below or in the SI.

The constraints on ω_n, $\vec{k}_n$, l_n, and s_n are given in the right column of Table I. This set of equations leads to the selection rules of nonlinear optics processes. The constraint on the spin, $s = \pm 1$, leads to selection rules on the polarization of the emitted photons [16,39–41], and the constraint of phase matching is important for interaction regions thicker than the coherence length. We shall now present a method to derive the PCLs, starting with the known ones and then two laws. The method is based on the superspace representation, which was developed in the context of quasicrystals [5]. The first step is to represent the driving field to superspace of N dimensions (as the number of N-photon types γ_n). Now, in the provided high enough dimensionality, a DS is guaranteed. Using this DS, we derive the selection rule. This selection rule is general since it is applicable for any driving field. We then formulate the general selection as an intuitive photonic conservation law.

We derive the selection rules from the symmetries according to Ref. [15], which reported a theory for multiscale dynamical symmetries and their selection rules. These multiscale symmetries consist of operations in time and in both microscopic and macroscopic space scales. Such a symmetry of the electric field, $\vec{E}$, can be described by

$$\vec{E}(\vec{X}) = \hat{\gamma}\vec{E}(\hat{\Gamma}\vec{X} + \vec{a}), \tag{2}$$

where $\vec{X}$ is the space-time vector and $\vec{a}$ is the macrospace-time translation vector. $\vec{X}$ and $\vec{a}$ can be vectors in the physical space or in the superspace (see Sec. 5 of SM [38]). $\hat{\gamma}$ is a microscopic operation, and $\hat{\Gamma}$ is a point-group operation in macrospace-time. As shown in Ref. [15], harmonic generation in an isotropic medium with a pump exhibiting the above multiscale dynamical symmetry, exhibits the following selection rule in Fourier domain (if $\vec{a}$ includes translation along the propagation axis, then reabsorption of the harmonics is neglected):

$$\hat{\gamma}\vec{F}(\hat{\Gamma}\vec{k})\exp(i\vec{k}\cdot\vec{a}) = \vec{F}(\vec{k}), \tag{3}$$

where $\vec{k}$ is the space-time wave vector and $\vec{F}(\vec{k})$ is the Fourier coefficient of the generated field, which is a complex-valued vector. In case of a discrete symmetry, Eq. (3) leads to

$$\phi_i(\vec{k}) = \vec{k}\cdot\vec{a} + \alpha_i + \phi_i(\hat{\Gamma}\vec{k}) - 2\pi Q, \tag{4}$$

where $\exp(i\alpha_i)$ is the ith eigenvalue of the microscopic operation, Q is an integer, and $\phi_i(\vec{k})$ is the phase of the Fourier coefficient $\vec{F}(\vec{k})$. In case of a continuous symmetry that involves microscopic rotation of $\delta\alpha$, macroscopic rotation of $\delta 2\pi lm/n$, and $\delta\vec{a}$ translation for any real number δ, Eq. (3) leads to

$$\vec{k}\cdot\vec{a} \pm \alpha + 2\pi lm/n = 0, \tag{5}$$

where l is the allowed winding number that characterizes the orbital angular momentum of the emitted $\vec{k}$ harmonic. Next, we apply the proposed method for deriving the selection rules in rows 1–3 in Table I. Consider a general field composed of superposition of monochromatic plane waves:

$$\vec{E}(t, X_1, X_2, \ldots, X_M) = \sum_{n=1}^{N}\vec{E}_n = \sum_{n=1}^{N}\vec{a}_n e^{i(\omega_n t + \sum_{m=1}^{M} k_{n,m}X_m)}, \tag{6}$$

where X_m are M different orthogonal space dimensions (physically, it is always the case that $M = 3$; however, M is effectively smaller in most experimental realizations, e.g., for plane-wave $M = 1$), and ω_n and $k_{n,m}$ are the angular frequency and wave vector of $\vec{E}_n$, respectively. For transforming into a superspace representation, we add more dimensions such that the field will be periodic for any combinations of ω_n and $k_{n,m}$. The field in superspace is given by

$$\vec{E}(t_1, t_2, \ldots, t_N, X_{1,1}, X_{1,2}, \ldots, X_{2,1}, X_{2,2}, \ldots, X_{N,M}) = \sum_{n=1}^{N}\vec{a}_n e^{i(\omega_n t_n + \sum_{m=1}^{M} k_{n,m}X_{n,m})}. \tag{7}$$

This field is periodic with respect to t_n with periodicity $2\pi/\omega_n$. Inserting the symmetry $t_n \rightarrow t_n + 2\pi/\omega_n$ into Eq. (4) with the translation vector $\vec{a} = \frac{2\pi}{\omega_n}\hat{t}_n$, where $\hat{t}_n$ is a unit vector along the t_n axis, and using the superspace wave vector $\vec{k}_S = \sum_{n=1}^{N}\omega_n^{(g)}\hat{t}_n + \sum_{m=1}^{M}\sum_{n=1}^{N}k_{n,m}^{(g)}\hat{X}_{n,m}$ where $\omega_n^{(g)}$ and $k_{n,m}^{(g)}$ are the generated temporal and spatial frequencies in superspace, gives

$$\begin{aligned}\phi_i(\vec{k}) &= \vec{k}_S\cdot\vec{a} + \alpha_i + \phi_i(\hat{\Gamma}\vec{k}) - 2\pi Q \\ &= \omega_n^{(g)}\frac{2\pi}{\omega_n} + \phi_i(\vec{k}) - 2\pi Q \\ \rightarrow \omega_n^{(g)} &= Q\omega_n = q_n\omega_n.\end{aligned} \tag{8}$$

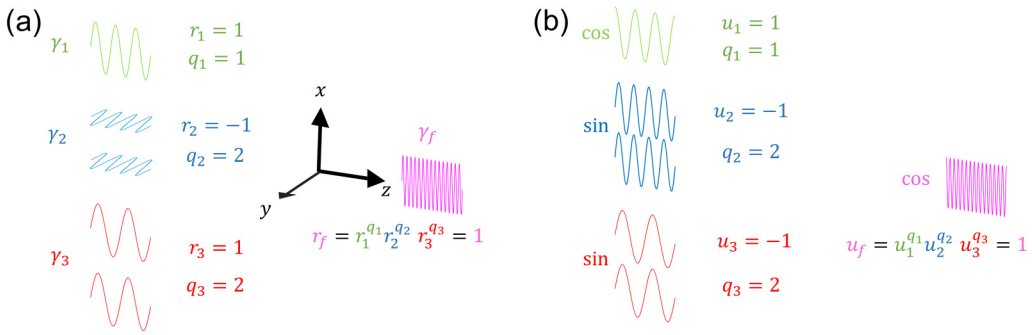

FIG. 1. Schematic illustrations of (a) conservation of reflection parity that is shown in row 6 in Table I and (b) space-time parity that is shown in row 7 in Table I.

Thus, the allowed frequencies along the $\hat{t}_n$ axis are harmonics of ω_n with q_n possible harmonics order. Hence, the allowed superspace temporal frequencies are any combination of q_n integers $\vec{\omega}_{\vec{q}} = \sum_{n=1}^{N} q_n \omega_n \hat{t}_n$. Projecting $\vec{\omega}_{\vec{q}}$ back to physical space ($t_n = t$), the allowed temporal frequencies are $\omega_{\vec{q}} = \sum_{n=1}^{N} q_n \omega_n$. Similar symmetry appears for each spatial coordinates, X_m, which leads to spatial harmonics, $k_{m\vec{q}_m} = \sum_{n=1}^{N} q_{n,m}\, k_{n,m}$. Next, we will show that $\vec{q}_m = \vec{q}$ by a symmetry that connects the spatial harmonics to the temporal harmonics. This is a continuous symmetry of $t_n \to t_n + \frac{\delta}{\omega_n}$ and $X_{n,m} \to X_{n,m} - \frac{\delta}{k_{n,m}}$ (i.e., $\vec{k} \cdot \vec{a} = \frac{\omega_n^{(g)}}{\omega_n} - \frac{k_{n,m}^{(g)}}{k_{n,m}}$), which according to Eq. (5),

$$\vec{k} \cdot \vec{a} = \frac{\omega_n^{(g)}}{\omega_n} - \frac{k_{n,m}^{(g)}}{k_{n,m}} = \frac{q_n \omega_n}{\omega_n} - \frac{q_{n,m} k_{n,m}}{k_{n,m}} = 0$$

gives the selection rule, $q_n - q_{n,m} = 0 \to q_n = q_{n,m}$. This important selection rule implies that the numbers of annihilated photons of each driver, with respect to energy and linear momentum (when X_m is in Cartesian coordinates) or orbital angular momentum (when X_m is the cylindrical angle in cylindrical coordinates), conservation rules are the same. Hence, we obtained rows 1–3 in Table I. Therefore, the allowed superspace wave vector of the emitted field is of the form

$$\vec{k}_S = \sum_{n=1}^{N} q_n \omega_n \hat{t}_n + \sum_{m=1}^{M} \sum_{n=1}^{N} q_n k_{n,m} \hat{X}_{n,m}. \tag{9}$$

The spin angular momentum (parity) conservation law in row 4 (5) in Table I is derived in Sec. 1 (3) of the SM.

Next, we derive the conservation law that is shown in row 6 of Table I [see also schematic illustration in Fig. 1(a)]. Consider a general EM field with polarization in the x-y plane, written here as a superposition of waves with x- or y-linear polarization:

$$\vec{E}(t, X_1, X_2, \ldots) = \hat{x} \sum_{n_x=1}^{N_x} a_{n_x} e^{i\left(\omega_{n_x} t + \sum_{m=1}^{M} k_{n_x,m} X_m\right)} + \hat{y} \sum_{n_y=1}^{N_y} a_{n_y} e^{i\left(\omega_{n_y} t + \sum_{m=1}^{M} k_{n_y,m} X_m\right)}. \tag{10}$$

This can be written in superspace as

$$\vec{E}(t_{1_x}, t_{2_x}, \ldots, t_{N_x}, t_{1_y}, t_{2_y}, \ldots, t_{N_y}, X_1, X_2, \ldots, X_M) = \hat{x} \sum_{n_x=1}^{N_x} a_{n_x} e^{i\left(\omega_{n_x} t_{n_x} + \sum_{m=1}^{M} k_{n_x,m} X_m\right)} + \hat{y} \sum_{n_y=1}^{N_y} a_{n_y} e^{i\left(\omega_{n_y} t_{n_y} + \sum_{m=1}^{M} k_{n_y,m} X_m\right)}. \tag{11}$$

This field has two discrete symmetries: (I) $t_{n_x} \to t_{n_x} + \frac{\pi}{\omega_{n_x}}$ for all $n_x = 1 \ldots N_x$ *simultaneously*, $\hat{\sigma}_x$. (II) $t_{n_y} \to t_{n_y} + \frac{\pi}{\omega_{n_y}}$ for all $n_y = 1 \ldots N_y$ *simultaneously*, $\hat{\sigma}_y$.

Therefore, according to Eq. (3) with $\vec{a} = \sum_{n_x=1}^{N_x} \frac{\pi}{\omega_{n_x}} \hat{t}_{n_x}$ for symmetry (I) and $\vec{a} = \sum_{n_y=1}^{N_y} \frac{\pi}{\omega_{n_y}} \hat{t}_{n_y}$ for symmetry (I) and $\vec{k}_S$ of Eq. (9), the Fourier domain of the generated field in the wave-mixing process must obey the following equations:

$$\hat{\sigma}_x \vec{F}(\vec{k}) \exp\left(i\pi \sum_{n_x=1}^{N_x} q_{n_x}\right) = \vec{F}(\vec{k})$$
$$\hat{\sigma}_y \vec{F}(\vec{k}) \exp\left(i\pi \sum_{n_y=1}^{N_y} q_{n_y}\right) = \vec{F}(\vec{k}), \tag{12}$$

which dictates that harmonics with odd $\sum_{n_x=1}^{N_x} q_{n_x}$ and even $\sum_{n_y=1}^{N_y} q_{n_y}$ are x-polarized harmonics with even $\sum_{n_x=1}^{N_x} q_{n_x}$ and odd $\sum_{n_y=1}^{N_y} q_{n_y}$ are y polarized, and all other harmonics are forbidden. This result is a photonic conservation law, which is an extension of parity conservation. We can associate this conserved quantity with the following conservation law: each photon carries a RP of $r = +1$ for an x-polarized photon or $r = -1$ for a y-polarized photon. The RP (i.e., the x- or y polarization) of the emitted photon is $r_f = \prod_n r_n^{q_n}$, which corresponds to the conservation of RP in the sixth row of Table I. Hence, all generated harmonic channels will be linearly polarized and will have phase differences between each other.

Last, we derive the conservation law in row 7 of Table I [see also schematic illustration in Fig. 1(b)]. Consider a general EM field, written here as superposition of cosine and sine waves with a linear polarization:

$$\vec{E}(t, X_1, X_2, \ldots) = \sum_{n_c=1}^{N_c} \vec{a}_{n_c} \cos\left(\omega_{n_c} t - \sum_{m=1}^{M} k_{n_c,m} X_m\right) + \sum_{n_s=1}^{N_s} \vec{a}_{n_s} \sin\left(\omega_{n_s} t - \sum_{m=1}^{M} k_{n_s,m} X_m\right), \tag{13}$$

where $\vec{a}_{n_c}$ and $\vec{a}_{n_s}$ are linearly polarized real-valued amplitudes. In superspace, we can write the field as

$$\begin{aligned}\vec{E}(t_{1_c}, t_{2_c}, \ldots, t_{N_c}, t_{1_s}, t_{2_s}, \ldots, t_{N_s}, X_1, X_2, \ldots, X_M) &= \sum_{n_c=1}^{N_c} \vec{a}_{n_c} \cos\left(\omega_{n_c} t_{n_c} - \sum_{m=1}^{M} k_{n_c,m} X_m\right) \\ &+ \sum_{n_s=1}^{N_s} \vec{a}_{n_s} \sin\left(\omega_{n_s} t_{n_s} - \sum_{m=1}^{M} k_{n_s,m} X_m\right).\end{aligned} \tag{14}$$

This field has a discrete symmetry, $t_{n_s} \to t_{n_s} + \frac{\pi}{\omega_{n_s}}$ for all $n_s = 1 \ldots N_s$ *simultaneously*, $\hat{I}$,where $\hat{I}$ is the STP operator (i.e., $\hat{I}\vec{E}(\vec{X}) = \vec{E}(-\vec{X})$). Hence, $\vec{a} = \sum_{n_s=1}^{N_s} \frac{\pi}{\omega_{n_s}} \hat{t}_{n_s}$ and $\hat{\Gamma}\vec{k} = \hat{I}\vec{k} = -\vec{k}$. Thus, inserting Eq. (4), the symmetry $t_{n_s} \to t_{n_s} + \frac{\pi}{\omega_{n_s}} \hat{I}$ gives

$$\begin{aligned}\phi_i(\vec{k}) &= \vec{k}_S \cdot \vec{a} + \alpha_i + \phi_i(\hat{\Gamma}\vec{k}) - 2\pi Q \\ &= \pi \sum_{n_s} q_{n_s} + \phi_i(-\vec{k}) - 2\pi Q \\ &\to \pi \sum_{n_s} q_{n_s} + \phi_i(-\vec{k}) - \phi_i(\vec{k}) = 2\pi Q,\end{aligned} \tag{15}$$

where $\phi_i(-\vec{k}) - \phi_i(\vec{k}) = 0$ for a generated cosine mode, and $\phi_i(-\vec{k}) - \phi_i(\vec{k}) = \pi$ for a generated sine mode. Therefore, for a generated sine mode in the induced polarization, $\sum_{n_s} q_{n_s}$ must be odd, and for a cosine mode, $\sum_{n_s} q_{n_s}$ must be even.

This result is a photonic conservation law, which is another extension to parity conservation. We can describe this law by considering photons that carry a STP, u, that equals 1 for cosine modes or -1 for sine modes. This STP is conserved such that the u_f of the emitted photon is $u_f = \prod_n u_n^{q_n}$, which corresponds to the conservation of the STP in the seventh row of Table I. Hence, all generated harmonic channels will be linearly polarized and will have phase differences between each other.

Numerical investigations. Below, we present numerical investigations of the selection rules that result from the developed PCL. These selection rules cannot result from the PCL in rows 1–5 in Table I. The single-atom HHG spectra are calculated using the strong-field approximation method [42] in two spatial dimensions, for an atom with a hydrogen-like dipole [43] and ionization potential of argon (15.76 eV), with the use of saddle-point approximation for momentum integrations and numerical integration in the ionization time domain.

Reflection parity conservation law (row 6 in Table I). Consider the driving field:

$$\vec{E}(t) = \sqrt{I_0} A(t)[\hat{x}\cos(\omega_1 t) + \hat{y}\cos(\omega_2 t + \phi)]. \tag{16}$$

The generated frequencies are $\omega_f = q_1\omega_1 + q_2\omega_2$. According to the RP conservation law, annihilation of odd q_1 and even q_2 photons leads to the emission of an $\hat{x}$-polarized photon, while annihilation of even q_1 and odd q_2 photons leads to the emission of a $\hat{y}$-polarized photon. We test this prediction numerally with $\omega_1 = 2.35 \times 10^{15}$ rad/s ($\lambda = 800$ nm) and $\omega_2 = \sqrt{2}\omega_1$ (and $\phi = 1$ rad), which allows us to easily identify the channel (q_1, q_2) corresponding to each spectral line in the emitted power spectrum. The amplitude envelope

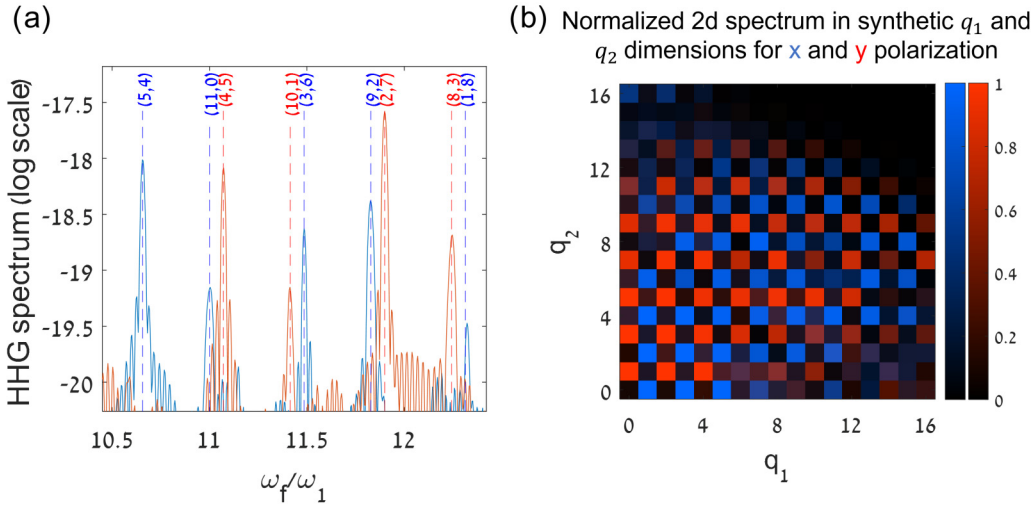

FIG. 2. (a) The power spectrum of x- (blue) and y- (red) linearly polarized harmonics driven by the field in Eq. (16), demonstrating the RP photonic law (row 6 in Table I) The polarization of the channels (q_1, q_2) predicted by the conservation law is displayed by the dashed lines. (b) The normalized power spectrum of x- (blue) and y- (red) linearly polarized harmonics driven by the field in Eq. (16) as a function of q_1 and q_2. As shown, the numerical results correspond well to the prediction.

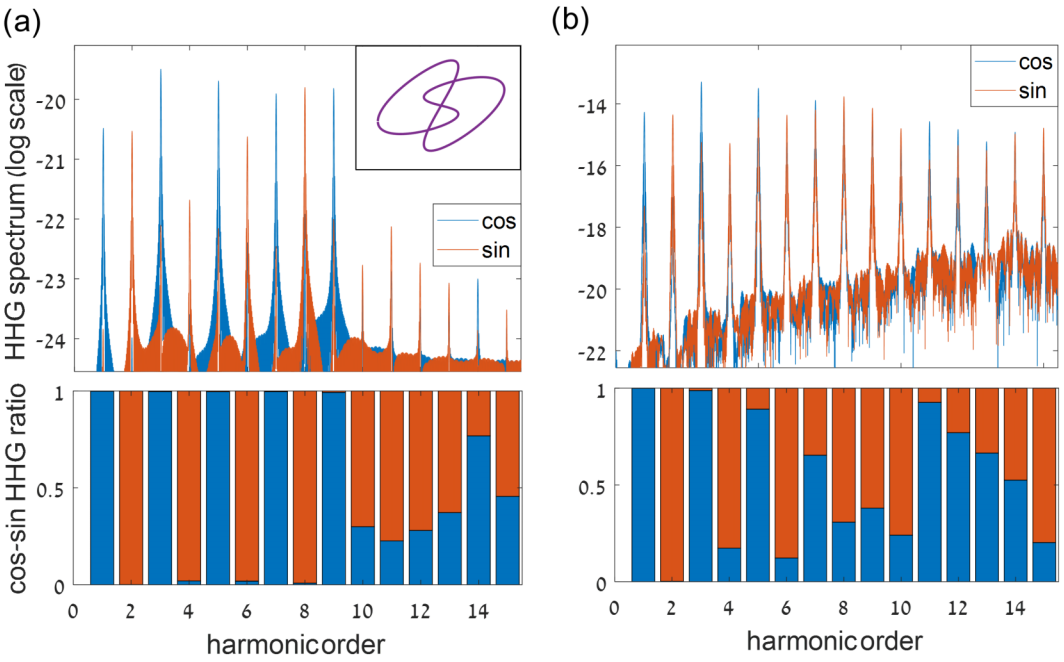

FIG. 3. Numerical investigation of the STP photonic law. (a) The Lissajous curve of the pump is plotted in the top right inset and is given in Eq. (17) with intensity, $\boldsymbol{I_0 = 10^{12}\ W/cm^2}$. The figure shows the power spectrum of high harmonics with cosine (blue) and sine (red) functions. The bottom plot shows the normalized relative power to the sine and cosine fields of each harmonic. As predicted by the conservation law, odd harmonics are cosine functions while even harmonics are sine. Harmonics beyond the cutoff exhibit significant deviations from the predicted conservation law. (b) Numerical investigation of the STP photonic law at relatively large ionization: The pump is the same as in (a), but with higher intensity, $\boldsymbol{I_0 = 10^{14}\ W/cm^2}$. The figure shows the power spectrum of high harmonics with cosine (blue) and sine (red) functions, showing that the STP is broken even for harmonics in the plateau.

is $A(t) = \exp(-(\frac{\omega_1}{2\pi\cdot 30}t)^6)$, and the peak intensity is $I_0 = 10^{14}$ W/cm^2.

As shown in Fig. 2, the polarizations of the numerically generated high harmonics agree with the prediction of the conservation law.

Space-time parity (row 7 in Table I). Consider the driving field:

$$\vec{E}(t) = \sqrt{I_0}A(t)[\hat{x}\cos(\omega_1 t) + \hat{y}\sin(\omega_2 t) + (0.5\hat{x} + \hat{y})\cos(\omega_3 t)]. \quad (17)$$

The generated frequencies are $\omega_f = q_1\omega_1 + q_2\omega_2 + q_3\omega_3$. According to the STP photonic law, when $q_1 + q_3$ is odd and q_2 is even, the harmonic field is proportional to $\cos(\omega_f t)$, while it is proportional to $\sin(\omega_f t)$ when $q_1 + q_3$ is even and q_2 is odd. We test this prediction numerally with $\omega_1 = 2.35 \times 10^{15}$ rad/s ($\lambda = 800$ nm), $\omega_2 = 2\omega_1$ and $\omega_3 = 3\omega_1$.The peak intensity is $I_0 = 10^{12}$ W/cm^2. In this case, all of the odd harmonics (of ω_1) are cosine functions, while all of the even harmonics are sine functions. We simulate the induced dipole as a function of time and then calculate the cosine (sine) harmonics by taking the real (imaginary) part of the Fourier transform of the induced dipole for both (arbitrary) orthogonal linear polarizations. The results are presented in Fig. 3(a), showing that harmonics in the plateau region indeed correspond to the predicted selection rule, up to deviations that are smaller than 0.1%.

Notably, time-reversal symmetry is broken by ionization process; hence, the STP photonic law, which results from time-reversal symmetry, is sensitive to ionization and is not perfectly upheld. To test this assumption, we increased the intensity of the driver field to $I_0 = 10^{14}$ W/cm^2. Now, as shown in Fig. 3(b), only harmonics 1–6 behave according to the conservation law, while the higher harmonics do not.

Discussion. To conclude, we explored here PCLs arising from symmetries in a superspace representation of the electromagnetic field interacting with matter, including two developed PCLs. These two laws describe the conservation of polarization-like properties of light, as well as its phaselike properties, and complement the well-established conservation of spin- and orbital angular momentum law. Beyond the development of the methodology and the derivation of PCLs, we highlight that our work assigns photonic characters associated with the PCL to electromagnetic waves, which should motivate future research to identify their origin and connection to other photonic characteristics.

Acknowledgment. This work was supported by the Israel Science Foundation (Grant No. 2626/23).

[1] R. W. Boyd, *Nonlinear Optics*, 3rd ed., Vol. 5 (Academic Press, Burlington, 2003).

[2] M. D. Perry and J. K. Crane, High-order harmonic emission from mixed fields, Phys. Rev. A **48**, R4051 (1993).

[3] J. B. Bertrand, H. J. Wörner, H. C. Bandulet, É. Bisson, M. Spanner, J. C. Kieffer, D. M. Villeneuve, and P. B. Corkum, Ultrahigh-order wave mixing in noncollinear high harmonic generation, Phys. Rev. Lett. **106**, 023001 (2011).

[4] G. Gariepy, J. Leach, K. T. Kim, T. J. Hammond, E. Frumker, R. W. Boyd, and P. B. Corkum, Creating high-harmonic beams with controlled orbital angular momentum, Phys. Rev. Lett. **113**, 153901 (2014).

[5] D. D. Hickstein, F. J. Dollar, P. Grychtol, J. L. Ellis, R. Knut, C. Hernández-García, D. Zusin, C. Gentry, J. M. Shaw, T. Fan, K. M. Dorney, A. Becker, A. Jaroń-Becker, H. C. Kapteyn, M. M. Murnane, and C. G. Durfee, Non-collinear generation of angularly isolated circularly polarized high harmonics, Nat. Photonics **9**, 743 (2015).

[6] L. Rego, J. S. Román, A. Picón, L. Plaja, and C. Hernández-García, Nonperturbative twist in the generation of extreme-ultraviolet vortex beams, Phys. Rev. Lett. **117**, 163202 (2016).

[7] A. Fleischer, O. Kfir, T. Diskin, P. Sidorenko, and O. Cohen, Spin angular momentum and tunable polarization in high-harmonic generation, Nat. Photonics **8**, 543 (2014).

[8] K. M. Dorney, L. Rego, N. J. Brooks, J. San Román, C.-T. Liao, J. L. Ellis, D. Zusin, C. Gentry, Q. L. Nguyen, J. M. Shaw, A. Picón, L. Plaja, H. C. Kapteyn, M. M. Murnane, and C. Hernández-García, Controlling the polarization and vortex charge of attosecond high-harmonic beams via simultaneous spin–orbit momentum conservation, Nat. Photonics **13**, 123 (2019).

[9] O. Kfir, P. Grychtol, E. Turgut, R. Knut, D. Zusin, D. Popmintchev, T. Popmintchev, H. Nembach, J. M. Shaw, A. Fleischer, H. Kapteyn, M. Murnane, and O. Cohen, Generation of bright phase-matched circularly-polarized extreme ultraviolet high harmonics, Nat. Photonics **9**, 99 (2014).

[10] O. Neufeld, D. Podolsky, and O. Cohen, Floquet group theory and its application to selection rules in harmonic generation, Nat. Commun. **10**, 405 (2019).

[11] C. L. Tang and H. Rabin, Selection rules for circularly polarized waves in nonlinear optics, Phys. Rev. B **3**, 4025 (1971).

[12] O. E. Alon, V. Averbukh, and N. Moiseyev, Selection rules for the high harmonic generation spectra, Phys. Rev. Lett. **80**, 3743 (1998).

[13] D. Baykusheva, A. Chacón, D. Kim, D. E. Kim, D. A. Reis, and S. Ghimire, Strong-field physics in three-dimensional topological insulators, Phys. Rev. A **103**, 023101 (2021).

[14] K. Chinzei and T. N. Ikeda, Time crystals protected by Floquet dynamical symmetry in Hubbard models, Phys. Rev. Lett. **125**, 060601 (2020).

[15] G. Lerner, O. Neufeld, L. Hareli, G. Shoulga, E. Bordo, A. Fleischer, D. Podolsky, A. Bahabad, and O. Cohen, Multiscale dynamical symmetries and selection rules in nonlinear optics, Sci. Adv. **9**, ade0953 (2023).

[16] O. Kfir, P. Grychtol, E. Turgut, R. Knut, D. Zusin, A. Fleischer, E. Bordo, T. Fan, D. Popmintchev, T. Popmintchev, H. Kapteyn, M. Murnane, and O. Cohen, Helicity-selective phase-matching and quasi-phase matching of circularly polarized high-order harmonics: Towards chiral attosecond pulses, J. Phys. B: At. Mol. Opt. Phys. **49**, 123501 (2016).

[17] E. Pisanty, G. J. Machado, V. Vicuña-Hernández, A. Picón, A. Celi, J. P. Torres, and M. Lewenstein, Knotting fractional-order knots with the polarization state of light, Nat. Photonics **13**, 569 (2019).

[18] E. Pisanty, L. Rego, J. San Román, A. Picón, K. M. Dorney, H. C. Kapteyn, M. M. Murnane, L. Plaja, M. Lewenstein, and C. Hernández-García, Conservation of torus-knot angular momentum in high-order harmonic generation, Phys. Rev. Lett. **122**, 203201 (2019).

[19] M. Luttmann, M. Vimal, M. Guer, J. F. Hergott, A. Z. Khoury, C. Hernández-García, E. Pisanty, and T. Ruchon, Nonlinear up-conversion of a polarization möbius strip with half-integer optical angular momentum, Sci. Adv. **9**, eadf3486 (2023).

[20] M. E. Tzur, O. Neufeld, E. Bordo, A. Fleischer, and O. Cohen, Selection rules in symmetry-broken systems by symmetries in synthetic dimensions, Nat. Commun. **13**, 1312 (2021).

[21] M. E. Tzur, O. Neufeld, A. Fleischer, and O. Cohen, Selection rules for breaking selection rules, New J. Phys. **23**, 103039 (2021).

[22] C. Hernández-García, A. Turpin, J. San Román, A. Picón, R. Drevinskas, A. Cerkauskaite, P. G. Kazansky, C. G. Durfee, and Í. J. Sola, Extreme ultraviolet vector beams driven by infrared lasers, Optica **4**, 520 (2017).

[23] F. Kong, C. Zhang, H. Larocque, Z. Li, F. Bouchard, D. H. Ko, G. G. Brown, A. Korobenko, T. J. Hammond, R. W. Boyd, E. Karimi, and P. B. Corkum, Vectorizing the spatial structure of high-harmonic radiation from gas, Nat. Commun. **10**, 2020 (2019).

[24] A. Forbes, M. de Oliveira, and M. R. Dennis, Structured light, Nat. Photonics **15**, 253 (2021).

[25] E. Frumker, N. Kajumba, J. B. Bertrand, H. J. Wörner, C. T. Hebeisen, P. Hockett, M. Spanner, S. Patchkovskii, G. G. Paulus, D. M. Villeneuve, A. Naumov, and P. B. Corkum, Probing polar molecules with high harmonic spectroscopy, Phys. Rev. Lett. **109**, 233904 (2012).

[26] D. Baykusheva, M. S. Ahsan, N. Lin, and H. J. Wörner, Bicircular high-harmonic spectroscopy reveals dynamical symmetries of atoms and molecules, Phys. Rev. Lett. **116**, 123001 (2016).

[27] S. Gholam-Mirzaei, J. Beetar, and M. Chini, High harmonic generation in ZnO with a high-power Mid-IR OPA, Appl. Phys. Lett. **110**, 061101 (2017).

[28] O. Neufeld, D. Ayuso, P. Decleva, M. Y. Ivanov, O. Smirnova, and O. Cohen, Ultrasensitive chiral spectroscopy by dynamical symmetry breaking in high harmonic generation, Phys. Rev. X **9**, 031002 (2019).

[29] D. Ayuso, O. Neufeld, A. F. Ordonez, P. Decleva, G. Lerner, O. Cohen, M. Ivanov, and O. Smirnova, Synthetic chiral light for efficient control of chiral light–matter interaction, Nat. Photonics **13**, 866 (2019).

[30] D. Ayuso, A. F. Ordonez, P. Decleva, M. Ivanov, and O. Smirnova, Enantio-sensitive unidirectional light bending, Nat. Commun. **12**, 3951 (2021).

[31] O. Neufeld and O. Cohen, Background-free measurement of ring currents by symmetry-breaking high-harmonic spectroscopy, Phys. Rev. Lett. **123**, 103202 (2019).

[32] D. Baykusheva and H. J. Wörner, Chiral discrimination through bielliptical high-harmonic spectroscopy, Phys. Rev. X **8**, 031060 (2018).

[33] G. Vampa, T. J. Hammond, M. Taucer, X. Ding, X. Ropagnol, T. Ozaki, S. Delprat, M. Chaker, N. Thiré, B. E. Schmidt,

F. Légaré, D. D. Klug, A. Y. Naumov, D. M. Villeneuve, A. Staudte, and P. B. Corkum, Strong-field optoelectronics in solids, Nat. Photonics **12**, 465 (2018).

[34] I. Tyulnev, Á. Jiménez-Galán, J. Poborska, L. Vamos, P. St. J. Russell, F. Tani, O. Smirnova, M. Ivanov, R. E. F. Silva, and J. Biegert, Valleytronics in bulk MoS_2 with a topologic optical field, Nature **628**, 746 (2024).

[35] S. Mitra, Á. Jiménez-Galán, M. Aulich, M. Neuhaus, R. E. F. Silva, V. Pervak, M. F. Kling, and S. Biswas, Light-wave-controlled Haldane model in monolayer hexagonal boron nitride, Nature **628**, 752 (2024).

[36] O. Neufeld, N. Tancogne-Dejean, U. De Giovannini, H. Hübener, and A. Rubio, Light-driven extremely nonlinear bulk photogalvanic currents, Phys. Rev. Lett. **127**, 126601 (2021).

[37] D. Shechtman, I. Blech, D. Gratias, and J. W. Cahn, Metallic phase with long-range orientational order and no translational symmetry, Phys. Rev. Lett. **53**, 1951 (1984).

[38] See Supplemental Material at http://link.aps.org/supplemental/10.1103/PhysRevResearch.6.L042034 for technical derivation of known conservation laws, and additional discussion on conservation laws and dynamical symmetries.

[39] T. Fan*et al.*, Bright circularly polarized soft x-ray high harmonics for x-ray magnetic circular dichroism., Proc. Natl. Acad. Sci. USA **112**, 14206 (2015).

[40] D. B. Milošević, Circularly polarized high harmonics generated by a bicircular field from inert atomic gases in the p state: A tool for exploring chirality-sensitive processes, Phys. Rev. A **92**, 043827 (2015).

[41] D. B. Milošević, High-order harmonic generation by a bichromatic elliptically polarized field: Conservation of angular momentum, J. Phys. B: At. Mol. Opt. Phys. **48**, 171001 (2015).

[42] M. Lewenstein, P. Balcou, M. Y. Ivanov, A. L'Huillier, and P. B. Corkum, Theory of high-harmonic generation by low-frequency laser fields, Phys. Rev. A **49**, 2117 (1994).

[43] H. A. Bethe and E. E. Salpeter, *Quantum Mechanics of One- and Two-Electron Atoms* (Springer, Berlin, 2013).